

# LATERAL TORSIONAL BUCKLING STRENGTH OF STEEL I-BEAMS WITH PREFLEXED BEAMS IN PRE-BENDING STAGE

Lin-jie Tian<sup>1</sup>, Zhe Li<sup>2</sup>, Ming Yang<sup>1,\*</sup>, Shan Chang<sup>1</sup> and Jian-qi Qian<sup>1</sup>

<sup>1</sup> School of Transportation, Southeast University, Nanjing, China

<sup>2</sup> Tongji Architectural Design(Group) Co., Ltd, Shanghai, China

\* (Corresponding author: E-mail: mingyang@seu.edu.cn)

## ABSTRACT

Attention should be paid to the lateral torsional buckling (LTB) of steel I-beams in pre-bending stage for the usage of preflexed beams. This paper develops analytical and numerical models for predicting LTB strength of steel I-beams arranged with different numbers of lateral braces and subjected to two movable concentrated loads in pre-bending stage. The different out-of-plane deformations of beam segments under assumed and actual conditions caused by bending moment distribution were considered, and the modified Rayleigh-Ritz method was proposed based on the constraint effect of adjacent beam segments. ABAQUS 2017 program was used for finite element analysis (FEA), and then have a comparison with the theoretical analysis. Additionally, LTB strength of steel I-beams with different parameters were investigated, and the effect of every selected parameter was described. The comparison results show that the modified Rayleigh-Ritz method has better applicability and accuracy under different parameters than the traditional Rayleigh-Ritz method, which can be used for selecting parameters and predicting LTB strength of steel I-beams in pre-bending stage.

## ARTICLE HISTORY

Received: 25 April 2019  
Revised: 20 October 2019  
Accepted: 24 October 2019

## KEYWORDS

Preflexed beam;  
Lateral torsional buckling;  
Modified Rayleigh-Ritz method;  
Lateral brace;  
LTB critical moment

Copyright © 2020 by The Hong Kong Institute of Steel Construction. All rights reserved.

## 1. Introduction

Preflexed beam was first proposed by Belgian bridge engineer A.Lipski around 1940s, which is widely used in South Korea, United States and other countries due to the advantages of convenient construction, light lifting, and low beam height. These beams are composed of steel I-beams, generally with symmetric or monosymmetric cross sections [1]. As shown in Fig.1, in order to make the concrete bottom flange prestressed, the steel I-beam is firstly preflexed by two concentrated loads, then concrete is cast around the bottom flange of the steel I-beam, after it has sufficiently hardened, the steel I-beam is unloaded with the concrete flange becomes prestressed subsequently.

As preflexed beam employed in more and more buildings and large span bridges, the concrete in compression area needs more compressive stress to improve its bearing capacity, which requires large concentrated loads in pre-bending stage [2]. However, lateral torsional buckling (LTB) usually occurs especially when the steel I-beam is slender enough (shown as Fig. 2). As one of the most effective ways, the longitudinal direction of the steel I-beams is usually set with discrete lateral braces to prevent this phenomenon (shown as Fig. 3).

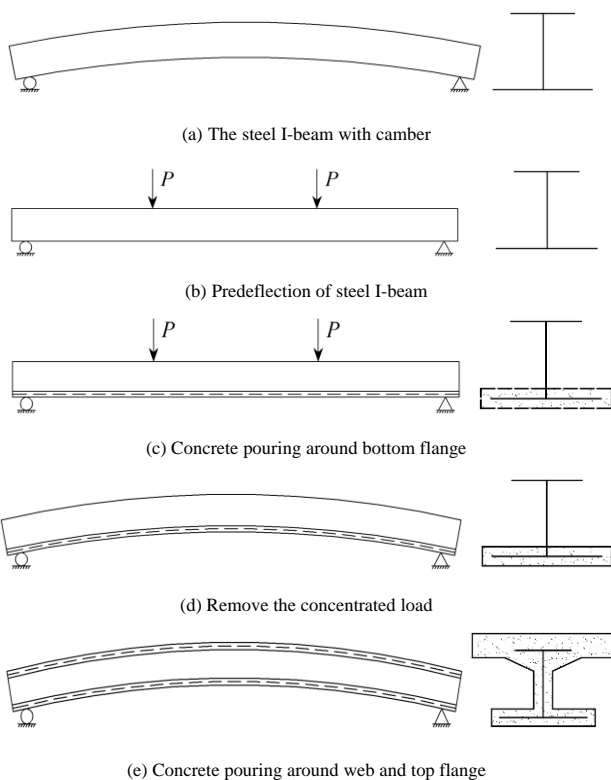


Fig.1 Construction process of preflexed beam



Fig. 2 LTB of the steel I-beam Fig. 3 Lateral braces of the steel I-beam

Considerable attention has been paid by researchers to study the LTB strength of steel I-beams. Some research on this issue are as follows: Taylor and Ojalvo [3] derived the exact solution for LTB strength of steel I-beams under uniform pressure, mid-span concentrated load and pure bending, respectively. Mutton et al. [4] studied the LTB strength of a simply supported steel I-beam under a central concentrated load arranged with a single brace at mid-span. Kitipornchai and Wang [5] investigated the LTB strength of simply supported steel I-beams with monosymmetric sections under moment gradient. Wang et al. [6] presented an automated Rayleigh-Ritz method for elastic buckling analysis of symmetric steel I-beams subjected to arbitrary loading condition. Nguyen et al. [7] studied the LTB strength of steel I-beams with discrete braces and then had a further study [8] on steel I-beams under various loading conditions. Gelera [9] analyzed the LTB strength of a steeped I-beam with singly symmetric cross sections. Ozbasaran et al. [10] proposed a closed-form equation to determine the LTB load, and an alternative design procedure was presented for predicting LTB strength of steel I-beams. Mohammadi et al. [11] investigated the LTB strength of steel I-beams with different degree of monosymmetry and web heights.

Few articles exist on steel I-beams subjected to two movable concentrated loads. In this study, steel I-beams arranged with different lateral bracing numbers and subjected to two movable concentrated loads were analyzed using traditional Rayleigh-Ritz method, and the modified Rayleigh-Ritz method was proposed based on the constraint effect of adjacent beam segments. Theory analysis and finite element analysis (FEA) were compared

under the most commonly used parameters for preflexed beams, and the effect of every selected parameter was investigated. The comparison results show that the finite element analysis results are in good agreement with the theoretical analysis results. In addition, the study of parameters can provide reference value for parameter selection of steel I-beams in pre-bending stage.

## 2. Theoretical Solution Based on Rayleigh-Ritz Method

Fig. 4(a) and Fig. 4(b) show two simply supported steel I-beams subjected to two movable concentrated loads without brace and with  $n$  lateral braces, respectively. The location of both of the concentrated loads are assumed at the distance of  $l/m$  from the beam ends, where  $l$  is the whole length of the steel I-beam, and the value of loading location parameter  $m$  can be optional, which denotes the loading location of concentrated loads.

It is assumed in Fig. 5(a) that  $x$ ,  $y$  and  $z$  axes denote strong axis, weak axis, and longitudinal axis of the steel I-beam, respectively. The  $u$ ,  $v$ , and  $w$  are designated for corresponding deformation of  $x$ ,  $y$  and  $z$ , respectively. The letter  $R$  in Fig. 4(b) represents the stiffness of lateral braces and the symbol  $\varphi$  in Fig. 5(b) represents the rotation angle of cross section. The point  $O$  and  $S$  in Fig. 5(b) stand for the centroid and the shear center of cross section, respectively.

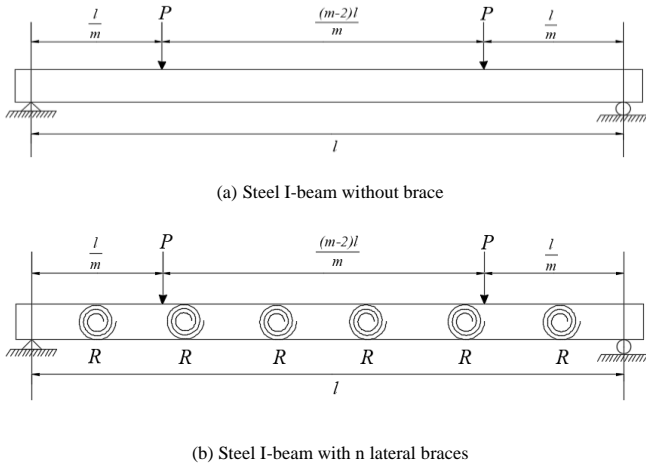
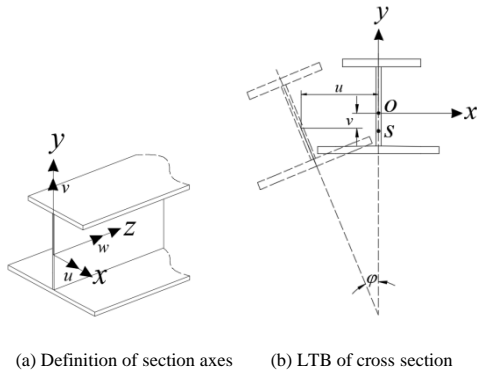
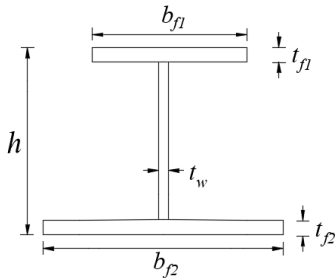


Fig.4 Theoretical calculation models of steel I-beams



(a) Definition of section axes (b) LTB of cross section



(c) Dimensions of cross section

Fig. 5 Cross section of the steel I-beam

of steel I-beams. The solution is derived based on the following assumptions: (a) the deformation in-plane can be ignored; (b) the material of the structure follows Hook' law; (c) the deformation of the member is small; (d) the contour of the cross section is rigid, (e) the elastic torsional braces are all set to centroidal axis; (f) the stiffness of the lateral braces  $R$  are all larger than or equal to bracing stiffness requirement  $R_T$ .

According to the above assumptions, the potential energy stored in steel I-beams without brace and with  $n$  lateral braces shown in Fig. 4(a) and Fig. 4(b) can be written as follows, respectively:

$$\begin{cases} U_0 = \frac{1}{2} \int_0^l [EI_y u''^2 + EI_w \varphi''^2 + (GI_t + 2\beta_y M_x) \varphi'^2 + 2M_x u'' \varphi] dz \\ U_n = \frac{1}{2} \int_0^l [EI_y u''^2 + EI_w \varphi''^2 + (GI_t + 2\beta_y M_x) \varphi'^2 + 2M_x u'' \varphi] dz + \frac{1}{2} R \sum_{i=1}^n \varphi_i^2 \end{cases} \quad (1)$$

Where  $E$  denotes the Young's modulus;  $I_y$  denotes the moment of inertia about weak axis;  $I_w$  denotes the warping constant;  $G$  denotes the shear modulus;  $I_t$  denotes the torsional constant;  $\beta_y$  denotes the monosymmetric property;  $M_x$  denotes the moment about strong axis of steel I-beams induced by concentrated load;  $\varphi_i$  ( $i=1,2,3,\dots,n$ ) denotes the twisting angle of cross section at lateral bracing points.

The energy increased by concentrated loads is:

$$\Omega = -\frac{1}{2} Pa [\varphi(l/m)]^2 - \frac{1}{2} Pa \left[ \varphi \left( \frac{m-1}{m} l \right) \right]^2 \quad (2)$$

Where  $P$  denotes the movable concentrated load;  $a$  denotes the distance of loading point above shear center.

Thus the total energy equations are obtained as follows from the sum of the above energy Eqs. (1) and (2):

$$\begin{cases} \Pi_0 = U_0 + \Omega \\ \Pi_n = U_n + \Omega \end{cases} \quad (3)$$

Where  $\Pi_0$  and  $\Pi_n$  are the total energy of steel I-beams without brace and with  $n$  lateral braces, respectively.

Based on the theory of material mechanics [12], the following equilibrium differential equation about the steel I-beam is obtained:

$$EI_y u'' = -M_x \varphi \quad (4)$$

For I-beams subjected to concentrated loads shown as Fig. 4(a) and Fig. 4(b), the functions about  $M_x$  are expressed as:

$$M_x = \begin{cases} Pz & 0 \leq z \leq \frac{l}{m} \\ \frac{Pl}{m} & \frac{l}{m} \leq z \leq \frac{(m-1)l}{m} \\ P(l-z) & \frac{(m-1)l}{m} \leq z \leq l \end{cases} \quad (5)$$

For a simply supported steel I-beam, there exists no torque, deflection, and bending moment at both beam ends. As a result, the boundary conditions are considered as follows:

$$u(0) = v(0) = w(0) = \varphi(0) = u''(0) = v''(0) = w''(0) = \varphi(l) = 0 \quad (6)$$

When no brace exists, the buckling model is a symmetric half-sine-wave, when the bracing stiffness is larger than the bracing stiffness requirement  $R_T$ , it will buckle in  $n+1$  model [13], so the twisting angle  $\varphi$  is assumed as follows which satisfies the above boundary conditions:

$$\begin{cases} \varphi_0(z) = C \sin\left(\frac{\pi z}{l}\right) & 0 \leq z \leq l \\ \varphi_n(z) = C \sin\left(\frac{(n+1)\pi z}{l}\right) & 0 \leq z \leq l, R \geq R_T \end{cases} \quad (7)$$

In this study, the Rayleigh-Ritz method was used to analyse LTB strength

Where  $\varphi_0(z)$  and  $\varphi_n(z)$  denote twisting angle of the steel I-beam without brace and with  $n$  lateral braces, respectively;  $C$  is the deformation coefficient of the steel I-beam deformed as the sine half-wave curve.

Substituting Eqs. (1), (2), (4), (5) and (7) into Eq. (3) yields the following equations:

$$\left\{ \begin{aligned} \Pi_0 &= \frac{1}{2} \int_0^l \left( \frac{\pi^4 E I_w}{l^4} C^2 \sin^2 \frac{\pi z}{l} + \frac{\pi^2 G I_t}{l^2} C^2 \cos^2 \frac{\pi z}{l} \right) dz \\ &+ \frac{1}{2} \int_0^l \left( \frac{2\pi^2 \beta_y M_x}{l^2} C^2 \cos^2 \frac{\pi z}{l} - \frac{M_x^2 C^2}{E I_y} \sin^2 \frac{\pi z}{l} \right) dz - P a k_0^2 C^2 \\ \Pi_n &= \frac{1}{2} \int_0^l \left( \frac{(n+1)^4 \pi^4 E I_w}{l^4} C^2 \sin^2 \frac{(n+1)\pi z}{l} + \right. \\ &\left. \frac{(n+1)^2 \pi^2 G I_t}{l^2} C^2 \cos^2 \frac{(n+1)\pi z}{l} \right) dz \\ &+ \frac{1}{2} \int_0^l \left( \frac{2(n+1)^2 \pi^2 \beta_y M_x}{l^2} C^2 \cos^2 \frac{(n+1)\pi z}{l} - \right. \\ &\left. \frac{M_x^2 C^2}{E I_y} \sin^2 \frac{(n+1)\pi z}{l} \right) dz - P a k_n^2 C^2 \end{aligned} \right. \quad (8)$$

Where  $k_0 = \sin(\pi/m)$ ,  $k_n = \sin[(n+1)\pi/m]$ .

According to the potential energy principle and the elastic stability theory of structure [13], the following equation is given as:

$$\frac{\partial \Pi_l}{\partial C} = 0 \quad (9)$$

Substituting Eq. (8) and  $P = mM/l$  into Eq. (9) leads to:

$$\left\{ \begin{aligned} M_{cr,0} &= \beta_1 \frac{\pi^2 E I_y}{l^2} \left\{ \left[ -\beta_2 a + \beta_3 \beta_y \right] + \sqrt{\left[ -\beta_2 a + \beta_3 \beta_y \right]^2 + \frac{I_w}{I_y} \left( 1 + \frac{l^2 G I_t}{\pi^2 E I_w} \right)} \right\} \\ M_{cr,n} &= \chi_1 \frac{\pi^2 E I_y}{l^2 (n+1)^2} \left\{ \left[ -\chi_2 a + \chi_3 \beta_y \right] + \sqrt{\left[ -\chi_2 a + \chi_3 \beta_y \right]^2 + \frac{I_w}{I_y} \left( 1 + \frac{l^2 (n+1)^2 G I_t}{\pi^2 E I_w} \right)} \right\} \end{aligned} \right. \quad (10a, b)$$

Where  $M_{cr,0}$  and  $M_{cr,n}$  represent the LTB critical moment of steel I-beams subjected to two movable concentrated loads without brace and with  $n$  lateral braces, respectively. And the functions of the parameters are expressed as follows:

$$\begin{aligned} \beta_1 &= \sqrt{\frac{6\pi t^2}{-8t^3 + 3\sin(2t) + 6\pi t^2 - 6t \cos 2t}}, \quad \beta_2 = \frac{2k^2}{\pi t} \beta_1, \\ \beta_3 &= \frac{\pi t - t^2 - \sin^2 t}{\pi t} \beta_1, \quad \chi_1 = \sqrt{\frac{6(n+1)\pi t_1^2}{-8t_1^3 + 3\sin(2t_1) + 6\pi t_1^2 - 6t_1 \cos 2t_1}}, \\ \chi_2 &= \frac{2k_n^2}{\pi t_1} \chi_1, \quad \chi_3 = \frac{\pi t_1 - t_1^2 - \sin^2 t_1}{\pi t_1} \chi_1, \quad k = \sin t, \\ t &= \frac{\pi}{m}, \quad k_1 = \sin t_1, \quad t_1 = \frac{(n+1)\pi}{m}. \end{aligned}$$

### 3. Modification of Rayleigh-Ritz Method

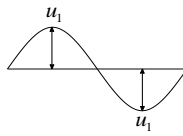
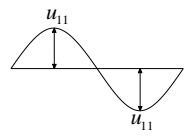
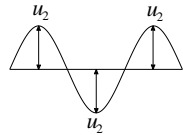
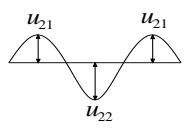
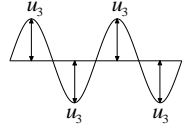
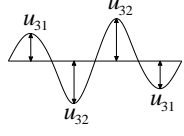
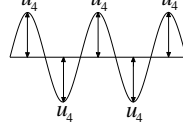
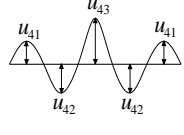
It should be noted that the derivation of the above equations of the steel I-beam with lateral braces are based on the assumption that the out-of-plane deformation distributes as the equal amplitude between the length of every brace [13]. However, for the steel I-beam subjected to two concentrated loads in pre-bending stage, the distribution of the out-of-plane deformation is unequal due to the influence of bending moment distribution, which is shown in Table 1.

In Table 1,  $u_n$  and  $u_{nj}$  represent the out-of-plane deformation of each steel I-beam segment distributed by  $n$  lateral braces under assumed and actual condition, respectively. Under actual condition, it is obvious that the out-of-plane deformation in the area of mid-span is larger than that of the beam ends. The larger the out-of-plane deformation of the adjacent beam segments is, the greater the constraint effects, which results that the LTB

critical moment  $M_{cr,n}$  (Eq. 10b) derived as the assumed condition is larger than the actual LTB critical moment of steel I-beams in pre-bending stage, and this result is disadvantageous to the stability of steel I-beams in pre-bending stage.

**Table 1**

Comparison of out-of-plane deformation between assumed and actual condition

The number of lateral braces	Out-of-plane deformation	
	Assumed condition	Actual condition
$n=1$		
$n=2$		
$n=3$		
$n=4$		

It is known that for a simply supported steel I-beam subjected to pure bending moment without brace, the LTB critical moment of the steel I-beam segment is provided as [14]:

$$M_{cr} = \beta_b \frac{\pi^2}{l_b^2} E I_y \left[ \beta_y + \sqrt{\beta_y^2 + \frac{I_w}{I_y} \left( 1 + \frac{l_b^2 G I_t}{\pi^2 E I_w} \right)} \right] \quad (11)$$

Where  $\beta_b$  is recommended by SSRC [15] as the following equation:

$$\beta_b = \frac{12.5 M_{\max}}{2.5 M_{\max} + 3 M_A + 4 M_B + 3 M_C} \quad (12)$$

Where  $M_{\max}$  is the maximum absolute moment value of the unbraced beam segment;  $M_A$ ,  $M_B$ ,  $M_C$  are the absolute values of moment at quarter, center, and three-quarter point, respectively.

As for Eq. (11),  $l_b$  is the length of unbraced beam segment;  $M_{cr}$  is the LTB critical moment of the unbraced beam segment which only considers the effect of pure bending, but ignores the constraint effect of adjacent beam segments due to the reason that there exists no lateral brace for the steel I-beam in the process of calculation. As a result, the provided LTB critical moment  $M_{cr}$  (Eq. 11) is smaller than the actual LTB critical moment of steel I-beams in pre-bending stage.

Compared with the actual LTB critical moment in pre-bending stage, the proposed LTB critical moment  $M_{cr,n}$  derived from Eq. (10b) is larger, while the provided LTB moment  $M_{cr}$  derived from Eq. (11) is smaller. In order to obtain the LTB critical moment of steel I-beams in pre-bending stage accurately, the modified combination coefficient  $\alpha = p\chi_1 + q\beta_b$  was proposed, and five different combinations of modified coefficients about  $p$  and  $q$  were analyzed based on seven cross section types shown in Table 2, and the relative errors of LTB critical moment between the results of theoretical calculation and FEA are shown in Tables 3(a), 3(b) and 3(c).

As shown in Table 2, Q345 was selected for all steel I-beams, the length of the steel I-beams were selected based on the specification that the maximum span of a single preflexed beam should not exceed 50m [16], and the other dimensions of cross sections were all selected according to the AISC

specification to prevent local buckling [14].

It is evident in Tables 3(a), 3(b) and 3(c) that when the number of lateral brace is constant, the relative errors produced by different combinations of modified coefficients show an increasing or decreasing trend. According to the comprehensive relative errors of all cross section types from A to G, when the coefficient combination is  $0.6\chi_1 + 0.4\beta_b$ , the standard deviation is 1.184, which is the smallest of all the modified coefficient combinations. Additionally, the relative errors of  $0.6\chi_1 + 0.4\beta_b$  are all less than 5%, which meet the calculation requirement of steel I-beams for the usage of preflexed beams (CJJ/T 276-2018, 2018). Therefore, the  $0.6\chi_1 + 0.4\beta_b$  is chose as the optimal modified coefficient combination in this study.

**Table 2**

Cross section types of steel I-beams

Cross	$l$ (m)	$h$	$b_{f1} = b_{f2}$ (mm)	$t_w$ (mm)	$t_{f1} = t_{f2}$ (mm)
A	20	600	350	15	20
B	25	700	400	18	22
C	30	900	560	22	28
D	35	1000	630	25	32
E	40	1200	750	30	38
F	45	1500	950	38	50
G	50	1700	1000	48	60

**Table 3(a)**

Relative errors of LTB critical moment (%)

Combination of modified coefficients	Cross section type E			Cross section type F			Cross section type G		
	$n=1$	$n=2$	$n=3$	$n=1$	$n=2$	$n=3$	$n=1$	$n=2$	$n=3$
$0.3\chi_1 + 0.7\beta_b$	0.96	-8.74	-3.45	1.36	-8.37	-2.58	1.24	-8.56	-3.34
$0.4\chi_1 + 0.6\beta_b$	1.01	-6.75	-1.21	1.4	-6.37	-0.32	1.28	-6.56	-1.1
$0.5\chi_1 + 0.5\beta_b$	1.05	-4.76	1.02	1.45	-4.37	1.93	1.32	-4.56	1.14
$0.6\chi_1 + 0.4\beta_b$	1.09	-2.77	3.26	1.49	-2.37	4.18	1.34	-2.03	3.37
$0.7\chi_1 + 0.3\beta_b$	1.13	-0.78	5.49	1.53	-0.37	6.44	1.41	-1.27	5.61

As a result, the optimal combination coefficient  $\alpha$ , shown as Eq. (13), is proposed to describe the constraint effect of beam segments, which can minimize the relative errors of LTB critical moments of steel I-beams between assumed and actual condition to the greatest extent:

$$\alpha = 0.6\chi_1 + 0.4\beta_b \quad (13)$$

Replacing  $\chi_1$  with  $\alpha$  for the LTB critical moment  $M_{cr,n}$ , then Eq. (10b) is amended as:

$$M'_{cr,n} = \alpha \frac{\pi^2 E I_y}{l^2 / (n+1)^2} \left\{ \left[ -\chi_2 a + \chi_3 \beta_y \right] + \sqrt{\left[ -\chi_2 a + \chi_3 \beta_y \right]^2 + \frac{I_w}{I_y} \left( 1 + \frac{l^2 / (n+1)^2 G I_1}{\pi^2 E I_w} \right)} \right\} \quad (14)$$

Where  $M'_{cr,n}$  represents the modified LTB critical moment of steel I-beam with  $n$  lateral braces, and subjected to two movable concentrated loads in pre-bending stage.

Thus, the bracing stiffness requirement  $R_T$  is presented by:

$$R_T = \frac{(M'_{cr,n}{}^2 - M_{cr,0}^2) l}{\beta_b^2 n E I_y} \quad (15)$$

## 4. Parameter analysis

### 4.1. FEA parameters

In this study, a plenty of three-dimensional finite element models were created using ABAQUS 2017 program based on different steel I-beam cross sections to verify the proposed modified Rayleigh-Ritz method. Shell element was used as the part of steel I-beams, and S4R element type was adopted for mesh generation. As shown in Fig. 6, reference points RP1 and RP2 were coupling constrained to the surfaces cut from the upper flange of the

**Table 3(a)**

Relative errors of LTB critical moment (%)

Combination of modified coefficients	Cross section type A			Cross section type B		
	$n=1$	$n=2$	$n=3$	$n=1$	$n=2$	$n=3$
$0.3\chi_1 + 0.7\beta_b$	0.17	-8.28	-2.51	-0.01	-8.67	-3.25
$0.4\chi_1 + 0.6\beta_b$	0.21	-6.27	-0.26	0.04	-6.67	-1.01
$0.5\chi_1 + 0.5\beta_b$	0.26	-4.27	2.00	0.08	-4.68	1.23
$0.6\chi_1 + 0.4\beta_b$	0.29	-2.27	4.26	0.12	-2.68	3.47
$0.7\chi_1 + 0.3\beta_b$	0.34	-0.26	6.52	0.16	-0.69	5.70

**Table 3(b)**

Relative errors of LTB critical moment (%)

Combination of modified coefficients	Cross section type C			Cross section type D		
	$n=1$	$n=2$	$n=3$	$n=1$	$n=2$	$n=3$
$0.3\chi_1 + 0.7\beta_b$	0.47	-8.75	-3.20	0.54	-8.86	-3.51
$0.4\chi_1 + 0.6\beta_b$	0.51	-6.76	-0.96	0.59	-6.87	-1.28
$0.5\chi_1 + 0.5\beta_b$	0.55	-4.77	1.28	0.63	-4.87	0.96
$0.6\chi_1 + 0.4\beta_b$	0.60	-2.78	3.53	0.67	-2.89	3.19
$0.7\chi_1 + 0.3\beta_b$	0.64	-0.79	5.76	0.71	-0.90	5.42

I-beam to avoid local stress concentration. Reference points RP3, RP4 and RP5 were created using "connect points to ground" type in ABAQUS 2017 Interaction module as lateral braces.

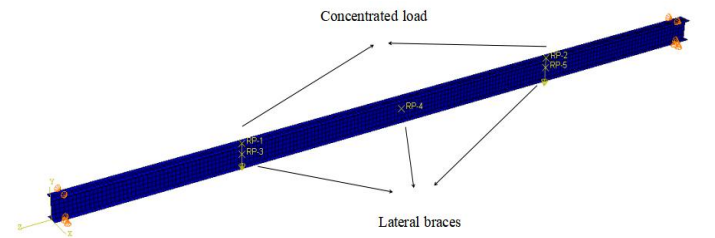


**Fig. 6** Finite element model of the steel I-beam

The boundary condition used for FEA was simply supported at both beam ends as shown in Fig.6. According to the principle that the error of finite element model calculation results of different density grids are less than 2% [17,18], the FEA models have been debugged repeatedly, and the seed spacing of 0.05m was selected to divide the grids, which can not only ensure the accuracy of simulation results but also save the calculation cost.

### 4.2. Case parameters

In this study, steel I-beams with symmetric and monosymmetric cross sections were selected to analyse and verify the proposed solution.

The dimensions of steel I-beams with symmetric sections are shown in Table 2. The length of steel I-beams with monosymmetric cross sections are 25m, the thickness of the top and bottom flange are 35mm, the thickness of web is 18mm, and the width of bottom flange is fixed at 400mm. The monosymmetric cross sections are vary with the value of the degree of monosymmetry  $\rho$ , which is calculated by:

$$\rho = \frac{I_{top}}{I_x} \quad (16)$$

Where  $I_{top}$  and  $I_x$  represent the moment of inertia of the top flange and the whole cross section of steel I-beams about strong axis, respectively. The shape of cross sections changed with  $\rho$  are shown in Table 4.

**Table 4**  
The shape of cross sections change with  $\rho$

The value of $\rho$	0.2	0.3	0.4	0.5	0.6	0.7	0.8
The shape of cross sections							

In order to verify the applicability of the proposed solution under different parameters, some research parameters commonly used for preflexed beams were selected according to CJJ/T 276-2018. The number of lateral braces  $n$  was set to 0,1,2, and 3, the high-span ratio of the steel I-beam  $\lambda$  was set to 0.02, 0.03, and 0.04, and the loading location parameter  $m$  was set to 3,4, and 5.

**5. Verification and parameter study**

*5.1. Verification of proposed solution*

*5.1.1. LTB critical moments of steel I-beams with symmetric cross sections*

In this section, a comparative analysis between the traditional and modified Rayleigh-Ritz method was conducted in order to verify the proposed solution, the number of lateral braces was set varied from 0 to 3, the most commonly used and studied high-span ratio  $\lambda=0.03$  and loading location parameter  $m=4$  was selected.

Table 5 shows the LTB critical moment values of steel I-beams with symmetric cross sections under different parameters in pre-bending stage. For all selected cross section types from A to G in Table 2, it can be seen that the relative errors between theoretical calculation and FEA are less than 2% when there exists no lateral brace or only one lateral brace is arranged. However, with the increase of lateral bracing number, the theoretical results calculated by traditional Rayleigh-Ritz method (Eq. 10b) become larger than the results of FEA, especially for  $n=3$ , the relative errors of all cross section types are larger than 10%. As a contrast, the results of modified Rayleigh-Ritz method (Eq. 14) are close to that simulated by FEA no matter how many lateral braces exist, when  $n=3$ , the relative errors are reduced by about 9% for all cross section types.

It is evident that the relative errors of modified Rayleigh-Ritz method are all less than 5%, which meet the calculation requirement of the standard (CJJ/T 276-2018, 2018), and it is accurate for predicting LTB strength of steel I-beams with symmetric cross sections in pre-bending stage.

*5.1.2. LTB critical moments of steel I-beams with monosymmetric cross sections*

As shown in Fig. 7(a), Fig. 7(b), Fig. 7(c), and Fig. 7(d), the LTB critical moments of steel I-beams with monosymmetric cross sections were analyzed to verify the modified Rayleigh-Ritz method.

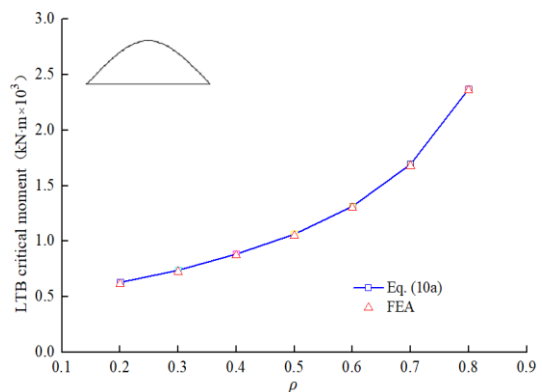
The results shown in Fig. 7(a) demonstrate that when no lateral brace exists, the traditional Rayleigh-Ritz method (Eq. 10a) and the FEA are in good agreement as  $\rho$  varied from 0.2 to 0.8. When there exists only one lateral brace, it can be seen from the detailed structure diagram of Fig. 7(b) that the results of Rayleigh-Ritz method after modification (Eq. 14) are closer to FEA than that before modification (Eq. 10b). As can be seen from Fig. 7(c) and Fig. 7(d), when there exist more than two lateral braces, the relative errors between Eq. (10b) and FEA become large with the increase of the value of  $\rho$  and the lateral bracing number, when  $n=3$  and  $\rho=0.8$ , the relative error is about 11.97%.

As is shown, the modified Eq.(14) is always well matched with the FEA as  $\rho$  varied from 0.2 to 0.8 and  $n$  varied from 0 to 3. When  $n=3$  and  $\rho=0.8$ , the relative error is reduced by 10.53%, about 1.44%. As a result, the modified Rayleigh-Ritz method has better accuracy than the traditional Rayleigh-Ritz method for predicting LTB strength of steel I-beams in pre-bending stage.

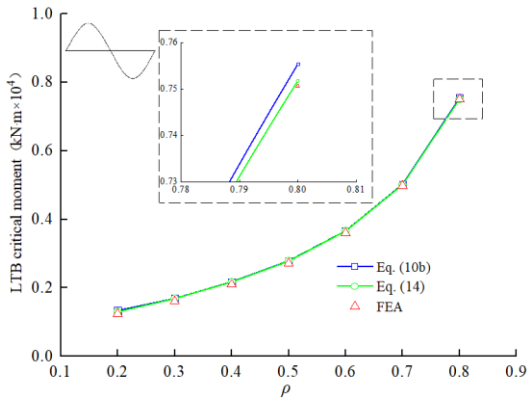
**Table 5**  
LTB critical moments of steel I-beams with symmetric cross sections

Cross section types	n	Eq. (10a,b) (kN·m)	Eq. (14) (kN·m)	FEA (kN·m)	Relative error between Eq. (10a, b) and FEA (%)	Relative error after modification(%)
A	0	368.2	-	375.4	-1.92	-
A	1	1091.0	1089.1	1085.9	0.47	0.29
A	2	2603.0	2405.8	2461.6	5.74	-2.27
A	3	4619.8	4251.7	4078.1	13.28	4.26
B	0	482.3	-	490.7	-1.71	-
B	1	1391.4	1389.1	1387.4	0.29	0.12
B	2	3263.1	3015.9	3099.1	5.29	-2.68
B	3	5746.5	5288.7	5111.5	12.72	3.47
C	0	1260.9	-	1271.2	-0.81	-
C	1	3931.0	3924.5	3901.0	0.77	0.60
C	2	9683.9	8929.4	9184.5	5.44	-2.78
C	3	17365.3	15981.9	15437.2	12.79	3.53
D	0	1766.6	-	1755.0	0.66	-
D	1	5370.0	5361.1	5325.4	0.84	0.67
D	2	13082.1	12026.5	12383.8	5.64	-2.89
D	3	23249.5	21397.3	20735.3	12.13	3.19
E	0	3122.1	-	3122.5	-0.01	-
E	1	9673.0	9656.9	9552.8	1.26	1.09
E	2	23742.6	21897.8	22521.1	5.42	-2.77
E	3	42525.4	39137.6	37903.0	12.20	3.26
F	0	7666.7	-	7615.0	0.68	-
F	1	24591.6	24550.7	24191.1	1.66	1.49
F	2	61340.0	56693.5	58069.7	5.63	-2.37
F	3	110919.3	102082.7	97982.8	13.20	4.18
G	0	11142.3	-	11073.8	0.62	-
G	1	33677.4	33621.1	33168.9	1.53	1.34
G	2	81334.2	75173.9	77153.1	5.42	-2.03
G	3	145118.0	133556.6	129201.5	12.32	3.37

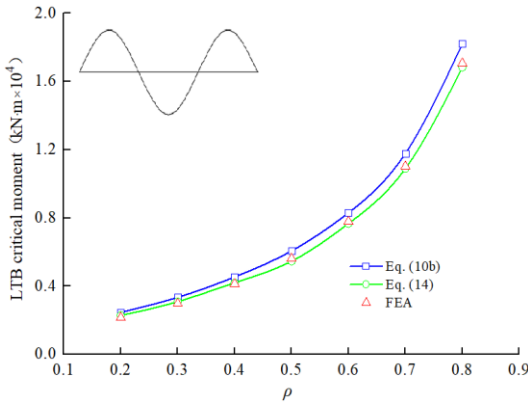
It can also be seen from Fig. 7 that with the increase of the value of  $\rho$ , LTB critical moments increase in concave parabola. Additionally, for the average value of LTB critical moments with all cross sections of  $\rho$  varied from 0.2 to 0.8, when the number of lateral braces changes from 0 to 1, the increase extent of LTB critical moments is the largest, about 2.77 times, followed by 2.08 times from 1 to 2, and the smallest from 2 to 3, about 1.87 times.



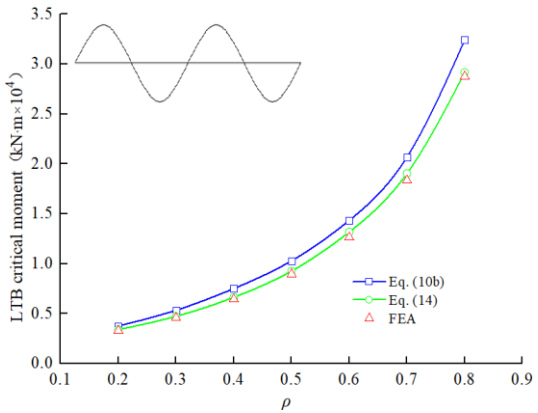
(a) LTB critical moments of steel I-beams without lateral brace



(b) LTB critical moments of steel I-beams with one lateral brace



(c) LTB critical moments of steel I-beams with two lateral braces



(d) LTB critical moments of steel I-beams with three lateral braces

Fig. 7 Comparison of LTB critical moments with different numbers of lateral braces

Therefore, the effect of increasing the LTB critical moment is not obvious with the increase of lateral bracing number, and it is necessary to arrange lateral braces rationally and economically according to reasonable calculation theory.

5.2. Effects of loading location parameter

In this section, a numerical study was done to analyse the LTB critical moment of steel I-beams under different loading location parameters as lateral bracing number varied from 1 to 3, and the high-span ratio  $\lambda$  was set to 0.03.

It is found according to the analysis results that the variation of LTB critical moments with different loading location parameters were similar for different values of  $\rho$ . As a result, LTB critical moments with the cross section of  $\rho = 0.5$  were selected as shown in Fig. 8.

Fig. 8 indicates that when  $n=1$ , the relative errors between traditional Rayleigh-Ritz method (Eq. 10b) and FEA are small, and the curves in Fig. 8 basically coincide.

When  $n=2$ , the relative errors are larger than that of  $n=1$ , as  $m=3$ , the relative error is 15.95%, and as  $m=5$ , the relative error is 4.18%, while the

relative errors between modified Rayleigh-Ritz method (Eq. 14) and FEA are 3.26% and -0.91%, respectively, the maximum relative error is reduced by 12.69%.

When  $n=3$ , the relative error before modification is the largest as  $m=3$ , about 15.84%, and the smallest as  $m=5$ , about 9.91%, while the relative errors after modification are 4.46% and 3.01% as  $m=3$  and  $m=5$ , respectively. As a result, the maximum relative error is reduced by 11.38%.

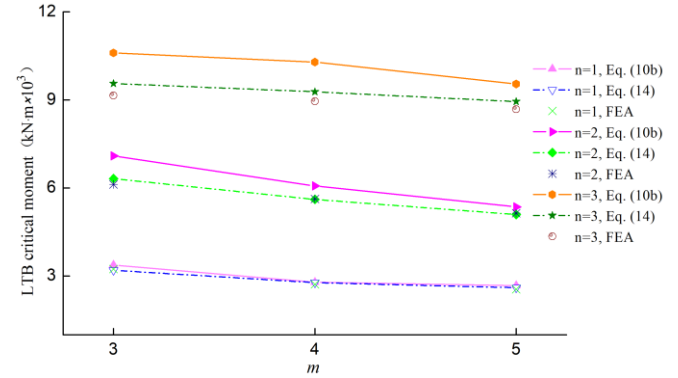


Fig. 8 Effects of different loading location parameters on LTB critical moment

It can be learned from Fig. 8 that the LTB critical moments of steel I-beams decrease with the increase of the value of  $m$ , and as the value of  $m$  decreases, the relative errors from the traditional Rayleigh-Ritz method increase, while the modified Rayleigh-Ritz method has good accuracy under different loading location parameters.

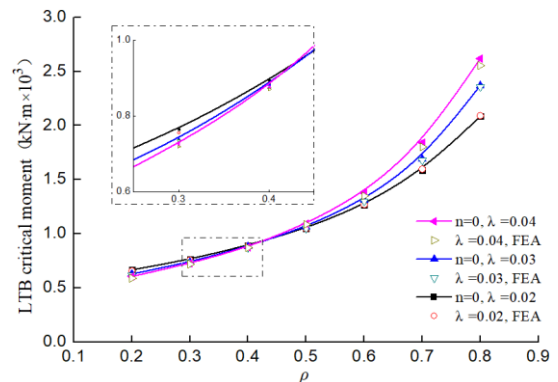
5.3. Effects of high-span ratio

In order to analyse the effects of different high-span ratios on LTB critical moments of steel I-beams in pre-bending stage, the high-span ratio  $\lambda$  in this section was set to 0.02, 0.03, and 0.04, the loading location parameter  $m$  was set to 4, and the proposed modified Rayleigh-Ritz method (Eq.14) was used to compare with the FEA.

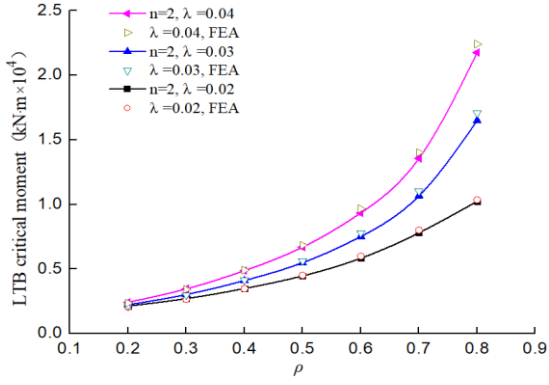
According to the theoretical calculation and FEA, it is concluded that the curves law of LTB critical moments change with  $\lambda$  as  $n=1$ ,  $n=2$  and  $n=3$  were similar. As a result, LTB critical moments change with different values of  $\lambda$  as  $n=0$  and  $n=2$  were selected for analysis as shown in Fig. 9(a) and Fig. 9(b).

It is found from the detailed structural diagram of Fig. 9(a) that when there is no lateral brace, for the cross section with the same value of  $\rho$ , when  $\rho < 0.5$ , LTB critical moment is larger as  $\lambda$  is smaller, however, when  $\rho \geq 0.5$ , LTB critical moment is larger as  $\lambda$  is larger. When  $\rho = 0.8$ , LTB critical moment is most affected by the value of  $\lambda$ , and as  $\lambda$  changes from 0.02 to 0.04, the LTB critical moment of the latter is 1.29 times of the former.

As a contrast, for steel I-beams with lateral braces, LTB critical moments increase with the increase of  $\lambda$  for all cross sections of  $\rho$  varied from 0.2 to 0.8, and LTB critical moments change significantly affected by different values of  $\lambda$  with the increase of  $\rho$ . As can be seen from Fig. 9(b), when  $n=2, \rho=0.8$ , as  $\lambda$  changes from 0.02 to 0.04, the LTB critical moment of the latter is 2.12 times of the former, which is much larger than that of  $n=0, \rho=0.8$ .



(a) LTB critical moments of steel I-beams without lateral brace



(b) LTB critical moments of steel I-beams with two lateral braces

Fig. 9 Effects of different high-span ratios on LTB critical moments

Therefore, it is necessary to select high-span ratio reasonably according to the value of  $\rho$  as well as whether the steel I-beam is arranged with lateral brace or not, so as to prevent the occurrence of LTB in pre-bending stage.

As can be seen from Fig. 9 that the results of modified Rayleigh-Ritz method are close to that of FEA for different high-span ratios as  $\rho$  varied from 0.2 to 0.8, which proves that the modified Rayleigh-Ritz method has good accuracy and applicability.

#### 5.4. Effects of stability coefficient

##### 5.4.1. The definition of stability coefficient of steel I-beams

This section aims to investigate the effects of stability coefficient of steel I-beams in pre-bending stage. For this purpose, the loading location parameter was set to 4, and the high-span ratio was set to 0.03. The stability coefficient  $\phi$  is defined as the ratio of  $M'_{cr,n}$  (Eq. 14) to the design moment of the mid-span cross section  $M_d$  :

$$\phi = \frac{M'_{cr,n}}{M_d} \quad (17)$$

Where  $M_d$  is provided as:

$$M_d = \frac{P_0 l}{4} \quad (18)$$

Where  $P_0$  is the preflexed force with the loading location parameter  $m=4$ , which can be written as:

$$P_0 = \frac{4(\sigma_{con} - \sigma_z) I_s}{l_{ysu}} \quad (19)$$

Where  $\sigma_z$  is the maximum stress of mid-span cross section caused by gravity of steel I-beams;  $I_s$  is the moment of inertia of steel I-beam around its center of gravity axis;  $l_{ysu}$  is the distance between the neutral axis and the upper flange edge of steel I-beam;  $\sigma_{con}$  is the control stress of mid-span cross section of steel I-beam, which is given as:

$$\sigma_{con} \leq 0.75 f_y \quad (20)$$

##### 5.4.2. Effects of stability coefficient of steel I-beams

In this section, the modified Rayleigh-Ritz method was used to analyse the stability coefficients of steel I-beams with different numbers of lateral braces in pre-bending stage, and the results were shown in Fig. 10.

It can be observed from Fig. 10 that the variation of stability coefficients with different lateral bracing numbers are small when  $\rho=0.2$ , while there is a big increase when  $\rho=0.8$ . It is evident that the stability coefficients increase as the number of lateral brace increases, while as  $\rho < 0.5$ , this increasing trend is not obvious. Therefore, the stability coefficient is greatly affected by the number of lateral braces when the value of  $\rho$  is large enough.

It is recommended that the stability coefficient of steel I-beams should be

larger than 3.5 [2]. As shown in Fig. 10, for the steel I-beams selected in this paper, when, the steel I-beams with more than three lateral braces satisfy the requirement.

Therefore, it is important to set lateral braces reasonably for different types of steel I-beams according to theoretical calculation in pre-bending stage, and the modified Rayleigh-Ritz method with good accuracy and applicability verified above can provide reference value for theoretical calculation in pre-bending stage.

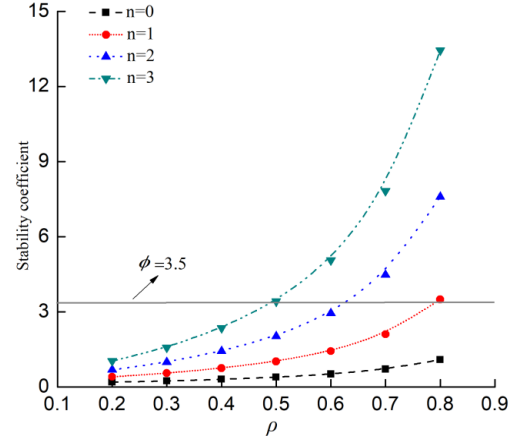


Fig. 10 Effects of stability coefficient

## 6. Summary and conclusions

In this research, in order to investigate the LTB strength of steel I-beams within preflexed beams in pre-bending stage, the steel I-beams subjected to two movable concentrated loads were analyzed. Due to the distribution of bending moment caused by concentrated loads, different combinations of modified coefficients were compared and analyzed, and the modified Rayleigh-Ritz method was proposed and verified under different parameters.

The LTB strength of steel I-beams with symmetric and monosymmetric cross sections show that the relative errors of traditional Rayleigh-Ritz method increase with the increase of the lateral bracing number, the degree of monosymmetry of the cross section, and the decrease of the value of loading location parameter. It is proved that the modified Rayleigh-Ritz method has good applicability and accuracy, which can provide theoretical calculation reference value for predicting LTB strength of steel I-beams in pre-bending stage.

Additionally, the parameter study in this paper can provide reference value for parameter selection of steel I-beams within preflexed beams in pre-bending stage.

## Acknowledgement

The financial support of Chinese National Natural Science Foundation (Grant No. 51078078) is gratefully acknowledged.

## References

- [1] Salvatore G. M. and Claudio M., "Preflex Beams: A method of calculation of creep and shrinkage effects", Journal of bridge engineering, 11(1), 48-58, 2006.
- [2] Huang Q., Design principle of bridge steel-concrete composite structure, China Communication Press, Beijing, China, 190-197, 2017. (in Chinese).
- [3] Taylor A.C. and Ojalvo M., "Torsional restraint of lateral buckling", Journal of the Structural Division, 92(2), 115-130, 1966.
- [4] Mutton B.C. and Trahair N.S., "Stiffness requirements for lateral bracing", Journal of the Structural Division, 99(10), 2167-2182, 1973.
- [5] Kitipornchai S. and Wang C.M., "Lateral buckling of tee beams under moment gradient", Computers & Structures, 23(1), 69-76, 1986.
- [6] Wang C.M., Wang L. and Ang K.K., "Beam-buckling analysis via Automated Rayleigh-Ritzmethod", Journal of Structural Engineering, 120(1), 200-211, 1994.
- [7] Nguyen C.T., Joo H.S., Moon J. and Lee H.E., "Flexural-torsional buckling strength of I-girders with discrete torsional braces under various loading conditions", Engineering Structures, 36(12), 337-350, 2012.
- [8] Nguyen C.T., Moon J., Le V.N. and Lee H.E., "Lateral-torsional buckling of I-girders with discrete torsional bracings", Journal of Constructional Steel Research, 66(2), 170-177, 2010.
- [9] Geleera K.M. and Park J.S., "Elastic lateral torsional buckling strength of monosymmetric stepped I-beams", KSCE Journal of Civil Engineering, 16(5), 785-793, 2012.
- [10] Ozbasaran H., Aydin R. and Dogan M., "An alternative design procedure for lateral torsional buckling of cantilever I-beams", Thin-Walled Structures, 90(1), 235-242, 2015.
- [11] Mohammadi E., Hosseini S.S. and Rohanimanesh M.S., "Elastic lateral-torsional buckling

- strength and torsional bracing stiffness requirement for monosymmetric I-beams”, *Thin-Walled Structures*, 104(3), 116-125, 2016.
- [12] Sun X.F., Fang X.S. and Guan L.T., *Mechanics of materials(I)*, Higher Education Press, Beijing, China, 157-175, 2008. (in Chinese).
- [13] Chen J., *Stability and steel structures theory and design*, Science Press, Beijing, China, 323-344, 2011. (in Chinese).
- [14] American Institute of Steel Construction, *Steel construction manual*, 14th Edition, Vol. 2, AISC, USA, 2011.
- [15] Structural Stability Research Council (SSRC), *Guide to stability design criteria for metal structures*, 5th Edition, Galambos. T.V., Wiley, New York, 1998.
- [16] CJJ/T 276-2018, *Technical standard for preflexed composite beam bridges*, Ministry of Housing and Urban-Rural Construction of the Republic of China, 2018. (in Chinese).
- [17] Cao J.F. and Shi Y.P., *FAQ Answers for ABAQUS Finite Element Analysis*, China Machine Press, Beijing, China, 130-156, 2008. (in Chinese).
- [18] ABAQUS (2017). “Standard user’s manual”, Version 6.17, Dassault Systemes, Paris.